Mon. Not. R. Astron. Soc. 000, 000–000 (2002) Printed 23 May 2002 (MN LaTeX style file v2.2)

High Mass X-ray Binaries as a Star Formation Rate Indicator in Distant Galaxies

H.-J. Grimm[1],M. Gilfanov[1,2],R. Sunyaev[1,2]
[1] Max-Planck-Institut für Astrophysik, 85741 Garching b. München, Germany
[2] Space Research Institute, Moscow, Russia

23 May 2002

ABSTRACT

Based on CHANDRA observations of nearby starburst galaxies and RXTE/ASM, ASCA and MIR-KVANT/TTM studies of high mass X-ray binary (HMXB) populations in the Milky Way and Magellanic Clouds, we propose that the number and/or the collective X-ray luminosity of HMXBs can be used to measure the star formation rate (SFR) of a galaxy. We show that, within the accuracy of the presently available data, a linear relation between HMXB number and the star formation rate exists. The relation between SFR and collective luminosity of HMXBs is non-linear in the low SFR regime, $L_X \propto \mathrm{SFR}^{\approx 1.7}$, and becomes linear only for sufficiently high star formation rate, when the total number of HMXB sources becomes sufficiently large. Such behaviour is caused by the fact, that we measure collective luminosity of a population of the discrete sources. Although more subtle SFR dependent effects are likely to exist, the data are broadly consistent with the existence of a universal luminosity function of HMXBs which can be roughly described as a power law with a differential slope of ~ 1.6, a cutoff at $L_X \sim$ few $\times 10^{40}$ erg/sec and a normalisation proportional to the star formation rate.

We apply our results to (spatially unresolved) starburst galaxies observed by CHANDRA at redshifts up to $z \sim 1$ in the Hubble Deep Field North and show that the calibration of the collective luminosity of HMXBs as a SFR indicator based on the local sample agrees well with the SFR estimates obtained for these distant galaxies with conventional methods.

Key words: Galaxies: starburst – X-rays: galaxies – X-rays: binaries

1 INTRODUCTION

X-ray observations open a new way to determine the star formation rate (SFR) in young very distant galaxies. CHANDRA observations of actively star forming galaxies in our vicinity and RXTE/ASM, ASCA and MIR-KVANT/TTM data about the high-mass X-ray binary (HMXB) populations in our Galaxy and Magellanic Clouds provide a possibility to calibrate the dependence of SFR on the X-ray luminosity of a galaxy due to HMXBs. For nearby, spatially resolved galaxies for which CHANDRA is able to resolve individual X-ray binaries we also have the opportunity to calibrate the dependence of SFR on the total number of X-ray sources.

In the absence of bright AGN, the X-ray emission of a galaxy is known to be dominated by collective emission of its X-ray binary populations (see e.g. Fabbiano (1994)). The X-ray binaries, conventionally divided into low and high mass X-ray binaries consist of a neutron star or a black hole accreting from a normal companion star. To form a NS or BH the initial mass of the progenitor star must exceed ~ 8 $M_\odot$ (Verbunt & van den Heuvel 1994). The main distinction between LMXBs and HMXBs is the mass of the optical companion with a broad, thinly populated dividing region between $\sim 1-5$ $M_\odot$. This difference results in drastically different evolution time scales for low and high mass X-ray binaries and, hence, different relations of their number and collective luminosity to the instantaneous star formation activity and the stellar content of the parent galaxy. In the case of a HMXB, having a high mass companion, generally $M_{optical} \gtrsim 10$ $M_\odot$ (Verbunt & van den Heuvel 1994), the characteristic time scale is at most the nuclear time scale of the optical companion which does not exceed $\sim 2 \cdot 10^7$ years whereas for a LMXB, generally $M_{optical} \lesssim 1$ $M_\odot$, it is of the order of $\sim 10^{10}$ years.

HMXBs were first recognised as short living objects feeded by the gas supply of a massive star as a result of the discovery of Cen X-3 as an X-ray pulsar by UHURU in a binary system with a companion of more than 17 $M_\odot$ (Schreier et al. 1972), and the localisation and mass estimation of Cyg X-1 black hole due to a soft/hard state transition occurring simultaneously with a radio flare (Tananbaum et al. 1972) and following optical observations of a bright massive counterpart (Bolton 1972; Lyutyi et al. 1973). The prompt evolution of HMXBs makes them a potentially good tracer of the very recent star formation activity in a galaxy whereas, due to slow evolution, LMXBs display no direct connection to the present value of SFR. LMXBs rather are connected to the total stellar content of a galaxy determined by the sequence of the star formation episodes experienced by a galaxy during its lifetime (Ghosh & White 2001; Ptak et al. 2001; Grimm et al. 2002).

Regarding interacting galaxies, like Antennae, their dynamics provide an upper limit on the evolution and existence time of HMXBs since the tidal tails and wave patterns in which star formation is most vigorous are very short lived phenomena, of order a crossing time of interacting galaxies (Toomre & Toomre 1972; Eneev et al. 1973).

Several calibration methods are employed to obtain SFRs using UV, FIR and radio flux from distant galaxies. All these methods rely on a number of assumptions about the environment in the galaxy and suffer from severe uncertainties, e.g. the influence of dust and the shape of the initial mass function (IMF). An additional and independent calibrator might therefore become a useful method for determination of SFR. Such a method, based on the X-ray emission of a galaxy, might circumvent one of the main sources of uncertainty of conventional SFR indicators – absorption by dust and gas. Indeed, galaxies are mostly transparent to X-rays above about 2 keV, except for the densest parts of the most massive molecular clouds.

Existence of various correlations between X-ray and optical/far-infrared properties of galaxies has been noted and studied in the past. Based on Einstein observations of normal and starburst galaxies from the IRAS Bright Galaxy Sample, Griffiths & Padovani (1990) and David et al. (1992) found correlations between the soft X-ray luminosity of a galaxy and its far-infrared and blue luminosity. Due to the limited energy range (0.5–3 keV) of the Einstein Observatory data one of the main obstacles in quantifying and interpreting these correlations was proper accounting for absorption effects and intrinsic spectra of the galaxies which resulted in considerable spread in the derived power law indices of the X-ray – FIR correlations, $\sim 0.7 - 1.0$. Although the X-ray data were not sufficient to discriminate between contributions of different classes of X-ray sources, David et al. (1992) suggested that the existence of such correlations could be understood with a two component model for X-ray and far-infrared emission from spiral galaxies, consisting of old and young populations of the objects having different relations to the current star formation activity in a galaxy. The uncertainty related to absorption effects was recently eliminated by Ranalli et al. (2002), who extended these studies to the harder energy band of 2–10 keV based on the BeppoSAX and ASCA data. In particular, they found a linear correlation between total X-ray luminosity of a galaxy and both radio and far-infrared luminosities and suggested that the X-ray emission might be directly related to the current star formation in the galaxy and that such a relation might hold also at higher redshifts.

The main surprise of the study presented here is that in the low SFR regime the relation between SFR and collective luminosity of HMXBs is non-linear, $L_X \propto \mathrm{SFR}^{\approx 1.7}$, and becomes linear only for sufficiently high star formation rate, when the total number of HMXB sources becomes sufficiently large. The non linear $L_X - SFR$ dependence is caused by the fact, that we measure collective luminosity of a population of the discrete sources. We give qualitative and approximate analytic treatment of this (purely statistical) effect below and will discuss it in more detail in a separate paper (Gilfanov et al. 2002).

There are, however, two main obstacles to use the X-ray luminosity of a galaxy as a SFR indicator. Firstly, if an active nucleus (AGN) is present in a galaxy it can easily outshine HMXB in X-rays. In principle, the presence of an AGN component might be identified and, in some cases separated, due to different X-ray spectra of an AGN and X-ray binaries, provided a sufficiently broad band energy coverage. Secondly, there is the dichotomy into LMXBs and HMXBs which both have somewhat similar spectra that also could probably be distinguished with sufficiently broad band coverage. To estimate the SFR one is interested only in the luminosity of HMXBs, therefore the LMXB contribution needs to be subtracted. This could, in principle, be done based on an estimate of the stellar mass of a galaxy. The results of a study of the X-ray binary population of our Milky Way (Grimm et al. 2002) and knowledge of the Galactic SFR allow to estimate at which point the emission of HMXBs dominates the emission of a galaxy. This obviously depends on the ratio of SFR to stellar mass of a galaxy. Roughly at a ratio of 0.005 $M_\odot$/yr per 10^{10} $M_\odot$ of total dynamical mass HMXB emission begins to dominate the X-ray emission. It should be emphasised, however, that even in the worst case the X-ray luminosity based SFR estimate should be able to provide an upper limit on the ongoing star formation activity in a galaxy.

Future observations with present and upcoming X-ray missions, especially Constellation-X and XEUS, the later having 1 arc sec angular resolution and a 100 times larger effective area than CHANDRA, will permit to get information about the SFR of galaxies from X-rays even at high redshifts. We know from optical and radio data that the SFR was much higher in galaxies at z $\sim$ 2–5 (Madau & Pozzetti 2000). Therefore we could expect that in these galaxies the contribution of HMXBs was strongly exceeding the contribution of LMXBs.

2 SAMPLE OF THE GALAXIES

For our analysis we chose a number of nearby late type/starburst galaxies observed by CHANDRA. We based our selection primarily on two criteria. Firstly, we selected galaxies that can be spatially resolved by CHANDRA sufficiently well so that the contribution of a central AGN can be discriminated and the luminosity functions of the compact sources can be constructed without severe confusion effects. However especially for galaxies farther away, like Antennae or NGC 3256, clustering of sources becomes more likely. Secondly, we limited our sample to galaxies known to have high star formation rates, so that the population of X-ray binaries is dominated by HMXBs and the contribution of low mass X-ray binaries can be safely ignored.

Table 1. The sample of local galaxies ordered according to SFR.

Source	Hubble type[(a)]	distance[(b)] [Mpc]	SFR [$M_\odot$/yr]	M [$10^{10} M_\odot$]	Ref.[(c)]	SFR/M [10^{-10}yr^{-1}]	$N(L > 2 \cdot 10^{38}$erg/s)	$L_{X,total}$ [10^{39} erg/s]	Ref.[(d)]
N3256	Sb(s) pec	35.0	44.0	5.0	(iii)	8.8	12	128	(3)
Antennae	Sc pec	19.3	7.1	8.0	(iii)	0.9	27	49	(4)
M 100	Sc(s)	20.4	4.8	24.0	(iv)	0.2	5	10	(5)
M 51	Sbc(s)	7.5	3.9	15.0	(vii)	0.26	15	16	(8)
M 82	Amorph	5.7	3.6	1.0	(ii)	3.6	12	23	(2)
M 83	SBc(s)	3.8	2.6	15.4	(vi)	0.17	2	0.14	(7)
N4579[(f)]	Sab(s)	23.5	2.5	-	-	-	5	26	(6)
M 74	Sc(s)	12.0	2.2	14.3	(i)	0.15	8	14	(1)
Circinus[(e)]	Sb	3.7	1.6	2.2	(vi)	0.73	6	5	(9)
N4736	RSab(s)	4.5	1.1	7.0	(vi)	0.16	4	4	(6)
SMC	Im	0.06	0.15	0.2	(viii)	0.75	1	0.4	(10)
Milky Way	SAB(rs)bc	-	0.25	54	(ix)	0.005	0	0.2	(11)

[(a)] from Sandage & Tammann (1980), except for Circinus.
[(b)] assuming $H_0 = 70$ km/s/Mpc and using velocities from Sandage & Tammann (1980).
[(c)] References for masses: (i) Sharina et al. (1996), (ii) Sofue et al. (1992), (iii) Lípari et al. (2000), (iv) Persic & Salucci (1988), (vi) Huchtmeier & Richter (1988), (vii) Kuno & Nakai (1997), (viii) Feitzinger (1980), (ix) Wilkinson & Evans (1999)
[d] References for X-ray observations: (1) Soria & Kong (2002), (2) Griffiths et al. (2000), (3) Lira et al. (2002), (4) Zezas et al. (2002), (5) Kaaret (2001), (6) Eracleous et al. (2002), (7) Soria & Wu (2002), (8) Terashima & Wilson (2002), (9) Smith & Wilson (2001), (10) Yokogawa (2002), (11) Grimm et al. (2002)
[(e)] velocity taken from de Vaucouleurs et al. (1991).
[(f)] We were not able to obtain a mass value for this source, but according to the rotation curve it is not much more massive than the Milky Way (Gonzalez Delgado & Perez 1996).

In order to probe the low SFR regime, we used the results of the X-ray binary population study in the Milky Way by Grimm et al. (2002), based on RXTE/ASM observations and the luminosity function of high mass X-ray binaries in the Small Magellanic Cloud obtained by ASCA (Yokogawa 2002).

The list of the galaxies selected along with their Hubble type, distances and other relevant parameters is given in Table 1.

2.1 Distances

To estimate X-ray luminosity and star formation rate, which is also based on flux measurements, and compare these values for different galaxies it is necessary to have a consistent set of distances. For the galaxies from our sample cosmological effects are not important. The distances were calculated using velocities from Sandage & Tammann (1980) corrected to the centre of mass of the Local Group and assuming a Hubble constant value of $H_0 = 70$ km/s/Mpc. The distances are listed in Table 1. Note that these distances might differ from the values used in the original publications on the X-ray luminosity functions and SFRs.

It is important to emphasise, that the uncertainty in the distances does not affect our main conclusion and the SFR–L_X calibration since, for small z, it has the same effect on the X-ray luminosity and SFR estimates from the conventional SFR indicators.

2.2 X-ray luminosity functions

For the X-ray luminosity functions we used published results of Chandra observations of late-type galaxies. References to the original publications are given in Table 1. The luminosity functions were rescaled to the distances described in the previous subsection. Note that, due to this correction, the total X-ray luminosities and luminosities of the brightest sources might differ from the numbers given in the original publications. The complete set of the luminosity functions for all objects from Table 1 is plotted in Fig. 1 (left panel).

One of the most serious issues important for the following analysis is the completeness level for the luminosity functions which is obviously different for different galaxies, due to different exposure times and distances. In those cases when the completeness luminosity was not given in the original publication, we used a conservative estimate based on the luminosity at which the luminosity function starts to flatten.

Due to the relatively small field of view of Chandra and sufficiently high concentration of X-ray binaries in the central parts of the galaxies the contribution of foreground and background objects can be neglected for the purpose of our analysis (e.g. M 51 (Terashima & Wilson 2002), M 83 (Soria & Wu 2002)).

The luminosities of the compact sources were derived in the original publications in slightly different energy bands, under different assumptions about spectral shape, and with different absorption column densities. Although all these assumptions affect somewhat the luminosity estimates, the resulting uncertainty is significantly smaller than those due to distance uncertainty and uncertainties in the star formation rate estimates. Therefore we make no attempt to correct for these differences.

2.3 Star formation rate estimates

One of the main uncertainties involved is related to the SFR estimates. The conventional SFR indicators rely on a number of assumptions regarding the environment in a galaxy, such as dust content of the galaxy, or the shape of the initial mass function (IMF). Although comparative analysis of different star formation indicators is far beyond the scope of

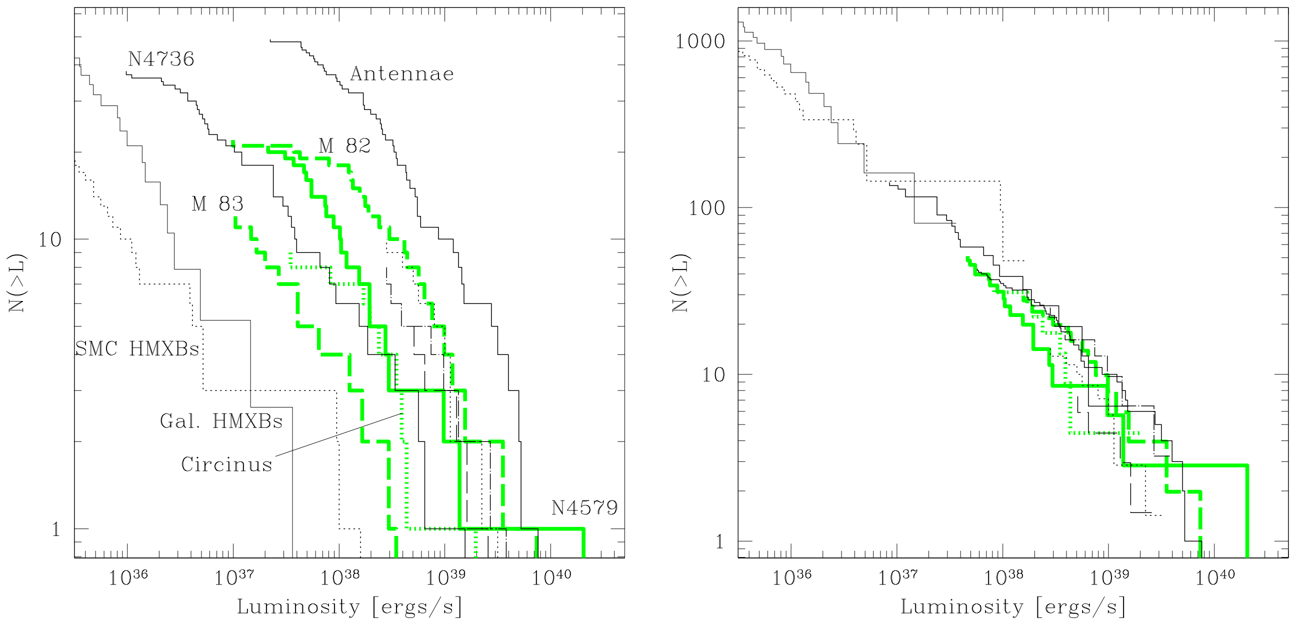

Figure 1. *Left:* The luminosity functions of compact X-ray sources in nearby galaxies listed in Table 1 obtained by CHANDRA. The luminosity functions are plotted assuming the distances from Table 1. *Right:* The luminosity functions for the same galaxies scaled by the ratio of their star formation rate to the SFR of Antennae. The luminosity functions in the right panel are plotted only above their corresponding completeness limits. It is clear that despite large differences in the SFRs (by a factor of $\sim 40-50$) the scaled luminosity functions occupy only a narrow band in the $N(>L)-L$ plane.

this paper, in order to roughly assess the amplitude of the uncertainties in the SFR estimates we compared results of different star formation indicators for each galaxy from our sample. For all galaxies except for Circinus we found measurements of at least 3 different star formation indicators in the literature, namely UV, H_α, FIR or thermal radio emission flux. The data along with the corresponding references are listed in Table 2.

In order to convert the flux measurements to star formation rates we use the result of an empirical crosscalibration of star formation rate indicators by Rosa-Gonzalez et al. (2002). The calibration is based on the canonical formulae by Kennicutt (1998) and takes into account dust/extinction effects. We used the following flux–SFR relations:

$$SFR_{H_\alpha} = 1.1 \cdot 10^{-41} \cdot L_{H_\alpha}[\mathrm{erg/s}] \quad (1)$$

$$SFR_{UV} = 6.4 \cdot 10^{-28} \cdot L_{UV}[\mathrm{erg/s/Hz}] \quad (2)$$

$$SFR_{FIR} = 4.5 \cdot 10^{-44} \cdot L_{FIR}[\mathrm{erg/s}] \quad (3)$$

$$SFR_{radio} = 1.82 \cdot 10^{-28} \cdot \nu_{\mathrm{GHz}}^{0.1} \cdot L_\nu[\mathrm{erg/s/Hz}] \quad (4)$$

The last relation is from Condon (1992) and applies only to the thermal radio emission, originating, presumably, in hot gas in HII regions associated with star formation (as we used thermal 1.4 GHz flux estimates from Bell & Kennicutt (2001)).

The above relations refer to the SFR for stars more massive than ~ 5 M$_\odot$. The total star formation rate, including low mass stars, could theoretically be obtained by extrapolating these numbers assuming an initial mass function – e.g. by a factor of ~ 20 for a Miller-Scalo IMF. Obviously, such a correction would rely on an assumption that the IMF does not depend on the initial conditions in a galaxy and would involve a significant additional uncertainty. On the other hand, this correction is not needed for our study as the binary X-ray sources, observed by CHANDRA harbour a compact object – a neutron star or a black hole, which according to the modern picture of stellar evolution can evolve only from stars with initial masses exceeding ~ 8 M$_\odot$. The SFR correction from $M > 5$ M$_\odot$ to $M > 8$ M$_\odot$ is relatively small ($\sim 20\%$) and, most importantly, due to the similarity of the IMFs for large masses it is significantly less subject to the uncertainty due to poor knowledge of the slope of the IMF. Thus, for the purpose of our study it is entirely sufficient to use the relations (1)–(4) without an additional correction. In the following, the term SFR refers to the star formation rate of stars more massive than ~ 5 M$_\odot$.

Since the relations (1)–(4) are based on the average properties of the star forming galaxies there is considerable scatter in the SFR estimates of a galaxy obtained using different indicators (Table 2). On the other hand, the SFR estimates based on different measurements of the same indicator are generally in a good agreement with each other. A detailed study, which SFR indicator is the most appropriate for a given galaxy is far beyond the scope of this paper. Therefore, we relied on the fact that for all galaxies from our sample, except Circinus, there are more than 3 measurements for different indicators. For each galaxy we disregarded the estimates significantly deviating from the majority of other indicators, and averaged the latter. The final values of the star formation rates we used in the following analysis are summarised in the last column of Table 2.

Table 2. The star formation rates for the galaxies from the local sample, measured by different SFR indicators.

Source	Fluxe					SFRs				
	UV[1]	H_α[2]	FIR[3]	radio[4]	Reference	UV	H_α	FIR	radio	adopted SFR
N3256		0.33	4.68		(i)		5.3	31.0		
			7.1		(j)			47.0		
			8.2		(h)			54.0		44
N4038/9		1.62			(a)		7.9			
(Antennae)	3.22	1.36	4.50	10.90	(b)	9.2	6.7	9.0	9.1	
			2.30		(d)			4.6		7.1
M 100		0.81			(a)		4.5			
	3.07	0.72	3.36		(b)	9.8	3.9	7.5		
			1.48		(d)			3.3		4.8
M 51	15.4	3.45	14.7	8.62	(b)	6.6	2.6	4.5	1.1	
		4.68			(a)		3.5			
		2.81			(c)		2.1			3.9
M 82		6.17	52.0		(e)		2.6	9.1		
		9.12			(a)		3.9			
	1.46	9.98	112.0	76.70	(b)	0.4	4.3	19.6	5.6	
			53.0		(d)			9.2		3.6
M 83		13.50			(f)		2.6			
		0.45			(g)		0.1			
	32.4	12.20	34.2		(b)	3.6	2.3	2.7		2.6
N4579		0.36			(f)		2.6			
		0.32			(a)		2.4			
			0.43		(d)			1.3		2.5
M 74		1.23			(a)		2.3			
	6.85	1.25	2.92		(b)	7.6	2.4	2.3		
		1.51			(c)		2.9			
			1.59		(d)			1.2		2.2
Circinus			223.0		(h)			1.6		1.6
N4736		5.37			(a)		1.6			
		5.37			(f)		1.6			
	6.49	2.10	6.78	5.80	(b)	1.1	0.6	0.8	0.3	1.1

Flux units: [1] – 10^{-25} erg/s/cm^2/Hz; [2] – 10^{-11} erg/s/cm^2; [3] – 10^{-9} erg/s/cm^2; [4] – 10^{-25} erg/s/cm^2/Hz

References: (a) Young et al. (1996), (b) Bell & Kennicutt (2001), (c) Hoopes et al. (2001), (d) David et al. (1992), (e) Armus et al. (1990), (f) Roussel et al. (2001), (g) Rosa-Gonzalez et al. (2002), (h) Negishi et al. (2001), (i) Buat et al. (2002), (j) Lípari et al. (2000)

2.4 Contribution of the central AGN

As mentioned in Sec. 1 the emission of a central AGN can easily outshine the contribution of X-ray binaries. However, due to the excellent angular resolution of CHANDRA it is possible to exclude any contribution from the central AGN in nearby galaxies. In our sample a central AGN is present only in the Circinus galaxy and NGC 4579 for which the point source associated with the nucleus of the galaxy was excluded from the luminosity function.

2.5 Contribution of LMXBs

Due to the absence of optical identifications of the donor star in the X-ray binaries detected by CHANDRA in other galaxies, except for LMC and SMC, there is no obvious way to discriminate the contribution of low mass X-ray binaries. On the other hand the relative contribution of LMXB sources can be estimated and, as it was mentioned above, it was one of the requirements to minimise the LMXB contribution, that determined our selection of the late-type/starburst galaxies.

Due to the long evolution time scale of LMXBs we expect the population of LMXB sources to be proportional to the stellar mass of a galaxy, whereas the population of the short living HMXBs should be defined by the very recent value of the star formation rate. Therefore the relative importance of LMXB sources should be roughly characterised by (inversely proportional to) the ratio of star formation rate to stellar mass of a galaxy. Since the determination of stellar mass, especially for a starburst galaxy, is very difficult and unsecure we used values for the total mass of a galaxy estimated from dynamical methods and assumed that the stellar mass is roughly proportional to the total mass. The values of the total mass, corresponding references, and the ratios of SFR to total mass are given in Table 1.

The SFR to total mass ratios for late type galaxies should be compared with that for the Milky Way, for which the population of sufficiently luminous X-ray binaries is studied rather well (Grimm et al. 2002). We know that the Milky Way, having a ratio SFR/M $\sim 5\cdot10^{-13}$ yr^{-1}is dominated by LMXB sources, the HMXB sources contributing $\sim 10\%$ to the total X-ray luminosity and $\sim 15\%$ to the total number (above $\sim 10^{37}$ erg/s) of X-ray binaries. As can be seen from Table 1, the minimal value of SFR/M $\sim 1.5\cdot10^{-11}$ yr^{-1} is achieved for M 74 and NGC 4736, which exceeds by a factor of ~ 30 that of the Milky Way. Therefore, even in the least favourable case of these two galaxies, we expect the HMXB sources to exceed LMXBs by a factor of ~ 3 at least, both in number and in luminosity. A more detailed comparison is shown in Fig. 2, where we plot the expected contributions of LMXBs and HMXBs to the observed luminosity

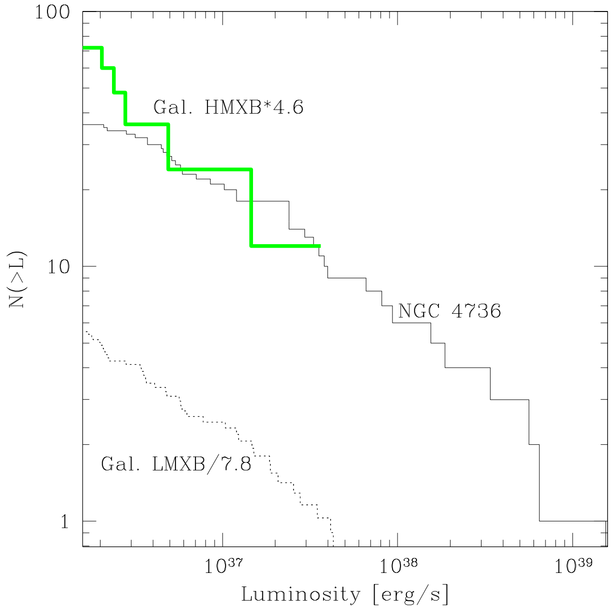

Figure 2. Contributions of LMXBs and HMXBs to the observed luminosity function for NGC 4736, having smallest SFR to total mass ratio (thin solid histogram). The upper thick grey histogram corresponds to the contribution of HMXBs scaled from the Milky Way HMXB luminosity function by the ratio of the SFRs. The lower dotted histogram is the Galactic LMXB luminosity function scaled by the ratio of the total masses. Total masses and SFRs are given in Table 1.

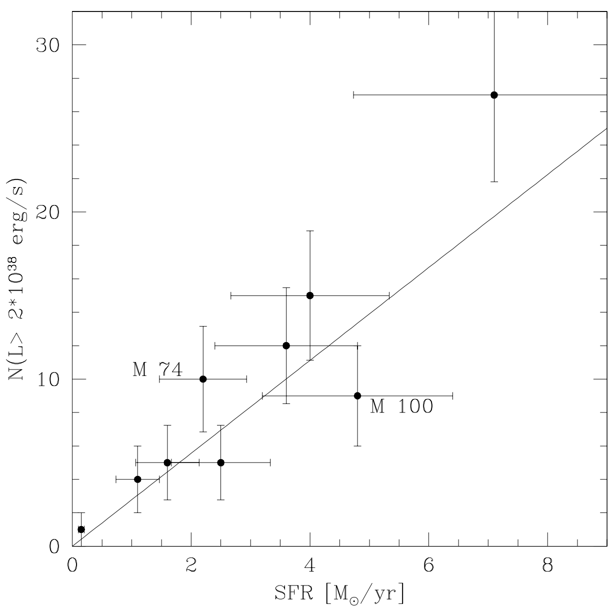

Figure 3. Number of sources with a 2–10 keV luminosity exceeding $2 \cdot 10^{38}$ erg/s versus SFR for galaxies from Table 1. The figure shows a clear correlation between the number of sources and the SFR. The straight line is the best fit from a Maximum-Likelihood, Eq. 5. The vertical error bars were calculated assuming a Poissonian distribution, the SFR uncertainty was assumed to be 30%. For M 74 and M 100, which completeness limit exceeds $2 \cdot 10^{38}$ erg/s the contribution of the sources below completeness limit was estimated from the "universal" luminosity function, Eq. 7.

function for NGC 4736. The luminosity function of HMXBs was obtained by scaling the Milky Way HMXB luminosity function by the ratio of SFRs of NGC 4736 to the Milky Way. The LMXB contribution was similarly estimated by scaling the Milky Way LMXB luminosity function by the ratio of the corresponding total masses. As can be seen from Fig. 2, the contribution of LMXB sources does not exceed $\sim 30\%$ at the lower luminosity end of the luminosity function. If the fractions of neutron stars and black holes in low mass systems in late-type/starburst galaxies are similar to that in the Milky Way, the contribution of the LMXBs should be negligible at luminosities above $\sim 10^{38}$ erg/sec, to which range most of the following analysis will be restricted.

3 HIGH MASS X-RAY BINARIES AS A STAR FORMATION INDICATOR

As already mentioned, the simplest assumption about the connection of HMXBs and SFR would be that the number of X-ray sources with a high mass companion is directly proportional to the star formation rate in a galaxy. In Fig. 1 (right panel) we show the luminosity functions of the galaxies from our sample scaled to the star formation rate of the Antennae galaxies. Each luminosity function is plotted above its corresponding completeness limit. It is obvious that after rescaling the luminosity functions, although not identical, occupy a rather narrow band in the log(N)-log(L) plane and seem to be consistent with each other within a factor of ~ 2 whereas the star formation rates differ by a factor of $\sim 40-50$. This similarity indicates that the number/luminosity function of HMXB sources might indeed be proportional to the star formation rate. This conclusion is further supported by Fig. 3 which shows the number of sources with a luminosity above $2 \cdot 10^{38}$ erg/s versus the SFR. The threshold luminosity was chosen at $2 \cdot 10^{38}$ erg/s to have a sufficient number of galaxies with a completeness limit equal or lower than that value and, on the other hand, to have a sufficient number of sources for each individual galaxy. In addition, as was discussed in Sec. 2.2, this choice of the threshold luminosity might help to minimise the contribution of LMXB sources. The errors for the number of sources were computed assuming a Poissonian distribution. For the SFR values we assumed a 30% uncertainty. Although the errors are rather big, the correlation of the number of sources with SFR is obvious. The slope of the correlation determined from a least-square fit in the form $N \propto SFR^{\alpha}$ is $\alpha = 0.97 \pm 0.07$, i.e. is consistent with unity. A fit of this correlation with a straight line $N \propto SFR$ (shown in the figure by solid line) gives:

$$N(L > 2 \cdot 10^{38}\mathrm{erg/s}) = (3.1 \pm 0.24) \cdot SFR[\mathrm{M}_{\odot}/\mathrm{yr}] \qquad (5)$$

According to this fit we should expect less than 1 source in the Milky Way, having a SFR of 0.25 $\mathrm{M}_{\odot}$/yr, which is in agreement with the fact that no sources above this luminosity are observed (Grimm et al. 2002).

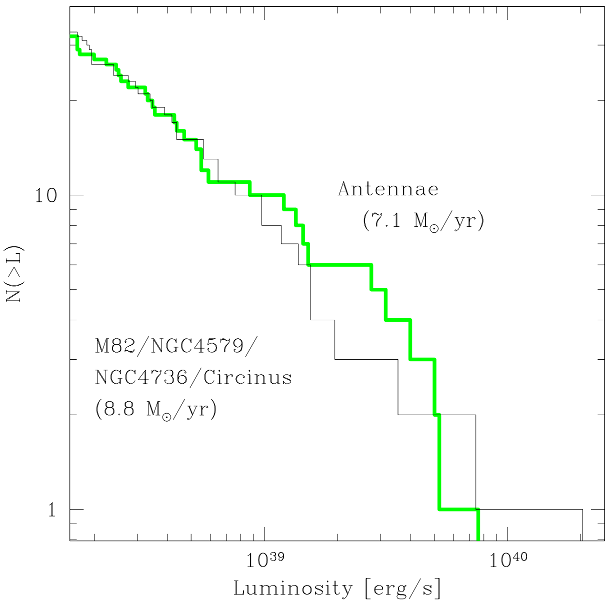

Figure 4. Comparison of the combined luminosity function of M 82, NGC 4579, NGC 4736 and Circinus, each having SFRs in the range 1–3.5 M$_\odot$/yr with Antennae luminosity function (7.1 M$_\odot$/yr). A Kolmogorov-Smirnov test gives a probability of 15% that the two luminosity functions are derived from the same distribution. See discussion in the text regarding the effect of the errors in the distance measurements on the shape of the combined luminosity function.

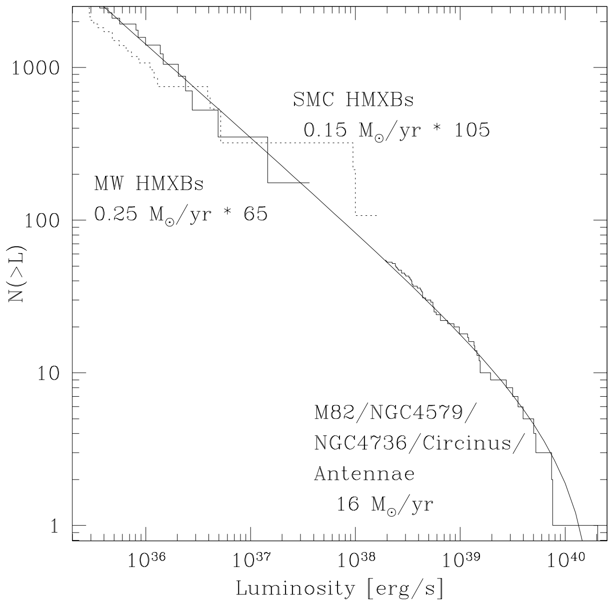

Figure 5. Combined luminosity function of compact X-ray sources in the starburst galaxies M82, NGC 4038/9, NGC 4579, NGC 4736 and Circinus with a total SFR of 16 M$_\odot$/yr (histogram above $2\cdot10^{38}$ erg/s) and the luminosity functions of HMXBs in the Milky Way and Small Magellanic Clouds (two histograms below $2\cdot10^{38}$ erg/s). The thin solid line is the best fit to the combined luminosity function of the starburst galaxies *only*, given by Eq. 7.

3.1 Universal HMXB Luminosity Function ?

In order to check the assumption that all the individual luminosity functions have identical or similar shape with the normalisation being proportional to the SFR, we compare the luminosity function of the Antennae galaxies, having a high star formation rate (~ 7 M$_\odot$/yr), with the collective luminosity function of galaxies with medium SFRs (in the range of ~ 1.0-3.5 M$_\odot$/yr). For the later we summed the luminosity functions of M 82, NGC 4579, NGC 4736 and Circinus, having a combined SFR of ~ 8.8 $M_\odot$/yr. The two luminosity functions (shown in Fig. 4) agree very well at $L_X \lesssim 10^{39}$ erg/s with possible differences at higher luminosities. In a strict statistical sense, a Kolmogorov-Smirnov test gives a 15% probability that the luminosity functions are derived from the same distribution, thus, neither confirming convincingly, nor rejecting the null hypothesis. However, it should be emphasised, that whereas the shape of a single slope power law luminosity function is not affected at all by the uncertainty in the distance, more complicated forms of a luminosity function, e.g. a power law with cut-off, would be sensitive to errors in the distance determination. The effect might be even stronger for the combined luminosity functions of several galaxies, located at different distances and each having different errors in the distance estimate. In the case of a power law with high luminosity cut-off, the effect would be strongest at the high luminosity end and will effectively dilute the cut-off, as probably is observed. Therefore, we can presently not draw a definitive conclusion about the existence of a universal luminosity function of HMXBs, from which all luminosity functions of the individual galaxies are strictly derived. For instance, subtle effects similar to the effect of flattening of the luminosity function with increase of SFR suggested by Kilgard et al. (2001); Ghosh & White (2001); Ptak et al. (2001) can not be excluded based on the presently available sample of galaxies and sensitivities achieved. We can conclude, however, that there is no evidence for strong non-linear dependences of the luminosity function on the SFR.

As the next step we compare the luminosity functions of actively star forming galaxies with that of low SFR galaxies. Unfortunately, the X-ray binary populations of low SFR galaxies is usually dominated by LMXB systems. One of the cases in which the luminosity function of HMXB sources can be reliably obtained is the Milky Way galaxy, for which all sufficiently bright X-ray binaries are optically identified. Another case is the Small Magellanic Cloud, which has a SFR value similar to our Galaxy, but is $\sim 300-500$ less massive and, correspondingly, has very few, if any, LMXB sources (Yokogawa 2002). Moreover, the SMC is close enough to have at least some optical identifications which makes a distinction like in the Milky Way possible. In order to do the comparison, we combined the luminosity functions of all actively star forming galaxies from our sample with a completeness limit lower than $2\cdot10^{38}$ erg/sec – M 82, Antennae, NGC 4579, NGC 4736 and Circinus. These galaxies have a total SFR of ~ 16 M$_\odot$/yr, which exceeds the Milky Way SFR (~ 0.25 M$_\odot$/yr) by a factor of ~ 65. Fig. 5 shows the combined luminosity function of the above mentioned star forming galaxies and the luminosity functions of the SMC and the Galactic HMXBs scaled according to the ratios of

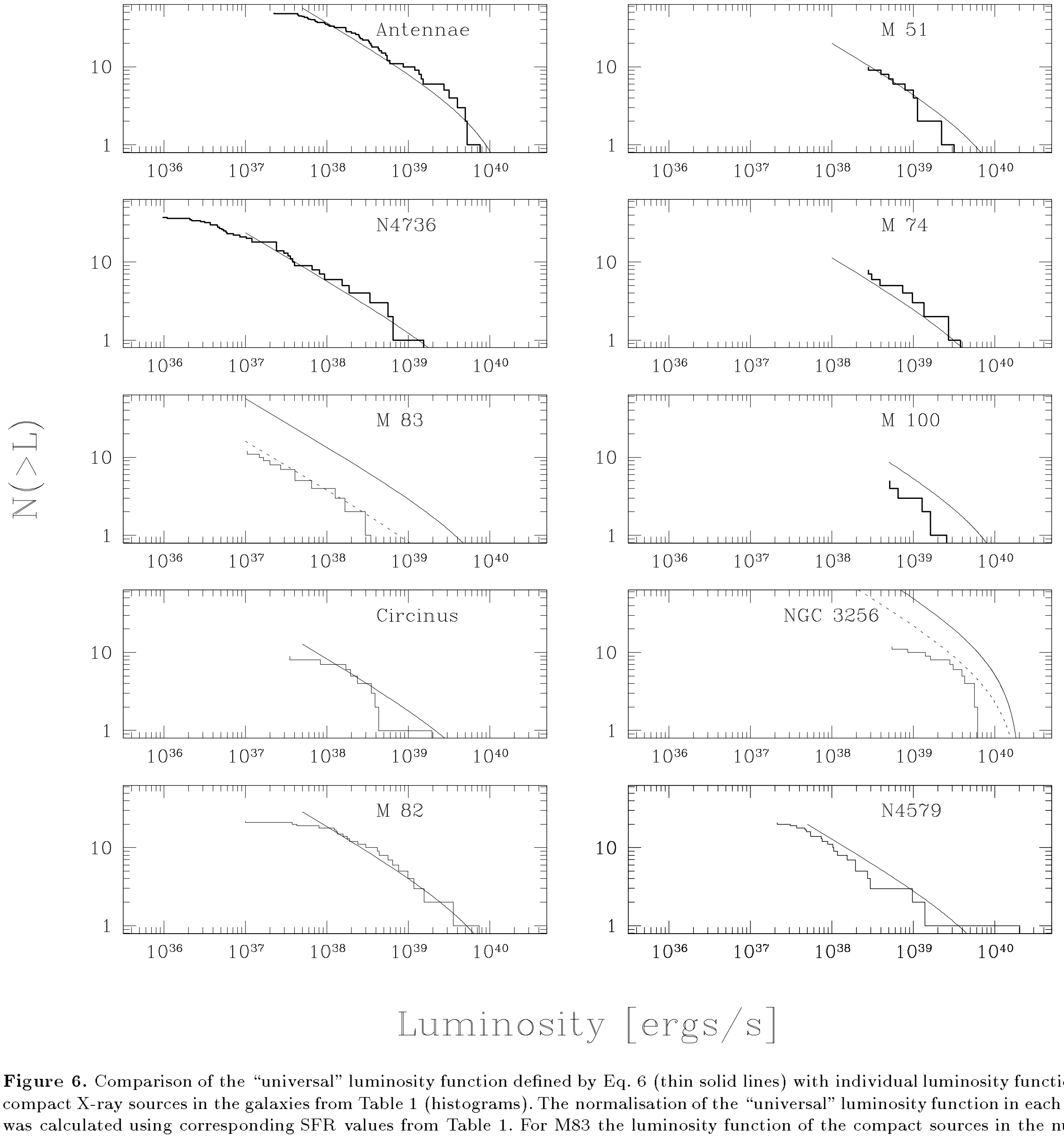

Figure 6. Comparison of the "universal" luminosity function defined by Eq. 6 (thin solid lines) with individual luminosity functions of compact X-ray sources in the galaxies from Table 1 (histograms). The normalisation of the "universal" luminosity function in each panel was calculated using corresponding SFR values from Table 1. For M83 the luminosity function of the compact sources in the nuclear region only is plotted, whereas the normalisation of the "universal" luminosity function was computed using the overall SFR for the galaxy. Therefore the thin line should be considered as an upper limit.

the SFRs. Shown in Fig. 5 by a solid line is the fit to the luminosity function of the high SFR galaxies *only* (see below), extrapolated to lower luminosities. It is obvious that the luminosity functions of Galactic and SMC HMXBs agree surprisingly well with an extrapolation of the combined luminosity function of the starburst galaxies.

Thus we demonstrated that the presently available data are consistent with the assumption that the approximate shape and normalisation of the luminosity function for HMXBs in a galaxy with a known star formation rate can be derived from a "universal" luminosity function whose shape is fixed and whose normalisation is proportional to the star formation rate. Due to a number of uncertainties involved, the accuracy of this approximation is difficult to assess. Based on our sample of galaxies we can conclude that it might be accurate within $\sim 50\%$.

In order to obtain the universal luminosity function of HMXBs we fit the combined luminosity function of M

82, Antennae, NGC 4579, NGC 4736 and Circinus using a Maximum-Likelihood method with a power law with a cut-off at $L_{max} = 2.1 \cdot 10^{40}$ erg/s and normalise the result to the combined SFR of the galaxies. The best fit luminosity function (solid line in Fig.5) in a differential form is given by:

$$\frac{dN}{dL_{38}} = 3.3 \cdot SFR \left[\frac{\mathrm{M}_\odot}{\mathrm{yr}}\right] \cdot L_{38}^{-1.6} \quad \text{for } L < L_{max}, \qquad (6)$$

and cumulative luminosity function:

$$N(>L) = 5.4 \cdot SFR \left[\frac{\mathrm{M}_\odot}{\mathrm{yr}}\right] \cdot (L_{38}^{-0.6} - 210^{-0.6}), \qquad (7)$$

where $L_{38} = L/10^{38}$ erg/sec.

As an additional test we checked all individual luminosity functions against our best fit using a Kolmogorov-Smirnov test. Taking into account the respective completeness limits, all individual luminosity functions are compatible with the assumption of a common 'origin'. In Fig. 6 we show the individual luminosity functions along with the universal luminosity function given by Eq.(6) with the normalisation determined according to the corresponding star formation rates.

3.2 High Luminosity cut-off

A notable feature of the combined luminosity function shown in Fig. 5 is the presence of a cut-off at $L_{max} \sim 2 \cdot 10^{40}$ erg/s. From the statistical point of view, when analysing the combined luminosity function of the high SFR galaxies only, the significance of the cut-off is not very high, with a single slope power law also giving an acceptable fit, although with lower probability according to a Kolmogorov–Smirnov test.

The existence of such a cut-off, if it is a universal feature of the HMXB luminosity function, can have significant implications to our understanding of the so called ultraluminous X-ray sources. Assuming that these very luminous objects are intermediate mass black holes accreting at the Eddington limit, the value of the cut-off gives an upper limit on the mass of the black hole, ~ 100 M$_\odot$. These apparently super-Eddington luminosities can also be the result of other effects, like beamed emission (King et al. 2001), or a strong magnetic field in neutron stars which may allow radiation to escape without interacting with the accreting material (Basko & Sunyaev 1976), or emission from a supercritical accretion disk (Shakura & Sunyaev 1973; Paczynsky & Wita 1980).

However, we can not exclude the possibility, that the cut-off is primarily due to the Antennae galaxies which contributes about half of the sources above 10^{39} erg/sec and shows a prominent cut-off in its luminosity function. On the other hand, further indication for a cut-off is provided by the luminosity function of NGC 3256. Conventional star formation indicators give for NGC 3256 value of SFR of ~ 45 $M_\odot$/yr however its luminosity function also shows a cut-off at $\sim 10^{40}$ erg/s. Unfortunately, due to the large distance (35 Mpc) and a comparatively short exposure time of the CHANDRA observation, ~ 28 ks, the luminosity function of NGC 3256 is complete only down to $\sim 6 \cdot 10^{39}$ erg/s which does not allow for a detailed investigation.

Another evidence for existence of a cut-off around $\sim$ few $\cdot\, 10^{40}$ erg/s is provided by the dependence of the collective luminosity of HMXB sources on the star formation rate discussed in the next subsections.

3.3 Total X-ray luminosity as SFR indicator

CHANDRA and future X-ray missions with angular resolution of the order of $\sim 1''$ would be able to spatially resolve X-ray binaries only in nearby galaxies ($d \lesssim \sim 50 - 100$ Mpc). For more distant galaxies only the total luminosity of a galaxy due to HMXBs can be used for X-ray diagnostics of star formation.

Fig. 7 shows the total luminosity of X-ray binaries (above 10^{36} erg/s) plotted versus SFR. The luminosities were calculated by summing the luminosities of individual sources down to the completeness limit of the corresponding luminosity function. The contribution of the sources below the completeness limit was approximately accounted for by integrating a power law distribution with slope 1.6 and normalisation obtained from the fit to the observed luminosity function. Note, that due to the shallow slope of the luminosity function the total luminosity depends only weakly on the lower integration limit.

As an additional data point we take luminosity and SFR for the Large Magellanic Cloud. The SFR is similar to the Milky Way SFR (Holtzman et al. 1999). Since no luminosity function is presently available for LMC we estimated it's integrated X-ray luminosity as a sum of the time averaged luminosities of the three brightest HMXB sources (LMC X-1, X-3, X-4) as measured by ASM (Grimm et al. 2002), $L_{2-10\ keV} \approx 3.4 \cdot 10^{38}$ erg/sec. Contribution of the weaker sources should not change this estimate significantly, since the luminosity of the next brightest source is by a factor of $\sim 30 - 50$ smaller (Syunyaev et al. 1990).

3.4 Theoretical $\mathrm{L_X}$–SFR relation

At first glance, the relation between collective luminosity of HMXBs and SFR can be easily derived integrating eq. (6) for the SFR dependent luminosity function. However it contains some subtleties related to the statistical properties of the power law distribution of the sources over luminosity, which appear not to have been recognised previously (at least in astrophysical context). As this effect might be of broader general interest and might work in many different situations related to computing/measuring integrated luminosity of a limited number of discrete objects, we give it a more detailed and rigorous discussion in a separate paper (Gilfanov et al. 2002), and restrict the discussion here to only a brief explanation and an approximate analytical treatment.

For illustration only, let us consider a population of discrete sources with a Gaussian luminosity function. As is well known, in this case sum of their luminosities – the integrated luminosity of the parent galaxy, also obeys a Gaussian distribution for which the mean luminosity and dispersion can be computed straightforwardly. An essential property of this simple case is that for an ensemble of galaxies, each having a population of such sources, the most probable value of the integrated luminosity of an arbitrarily chosen galaxy equals to the mean luminosity (averaged over the ensemble of galaxies). The situation might be different in the case of a population of discrete sources with a power law (or similar) luminosity function. In this case an ensemble of galaxies would have a non-Gaussian probability distribution of the integrated luminosity. Due to the skewness of the probability distribution in this case, the most probable value of the integrated luminosity of an arbitrarily chosen galaxy does not necessarily coincide with the mean value (the ensemble average). The effect is stronger for smaller number of sources and for flatter luminosity function. Of course, in the limit of large number of sources the distribution becomes asymptotically close to Gaussian and, correspondingly, the difference between the most probable value and the ensemble average vanishes and the relation between the integrated luminosity of HMXBs and SFR can be derived straightforwardly integrating eq.(6) for $L_{max} = 2.1 \cdot 10^{40}$ erg/s:

$$L_{2-10\ \mathrm{keV}} = 6.7 \cdot 10^{39} \cdot SFR[\mathrm{M}_\odot/\mathrm{yr}]\ \ \mathrm{erg/s} \qquad (8)$$

The ensemble average integrated luminosity is, of course, always described by the above equation, independently on the number of sources and shape of the luminosity function.

The following simple consideration leads to an approximate analytical expression for the most probable value of the integrated luminosity. Assuming a power law luminosity function $dN/dL = A \cdot SFR \cdot\ L^{-\alpha}$ with $1 < \alpha < 2$ and high luminosity cut-off at L_c, one might expect, that the brightest source would most likely have a luminosity L_{max} close to the value at which $N(> L_{max}) \sim 1$, i.e.

$$L_{max} \propto SFR^{\frac{1}{\alpha-1}} \qquad (9)$$

This value, of course, should not exceed the cut-off luminosity L_c. The most probable value of the total luminosity can be computed integrating the luminosity function from L_{min} to $\min(L_{max}, L_c)$:

$$L_{total} \approx \int_{L_{min}}^{\min(L_{max},L_c)} \frac{dN}{dL} L\, dL \qquad (10)$$

which leads to

$$L_{total} \approx \frac{A \cdot SFR}{2-\alpha} \cdot \min(L_{max}, L_c)^{2-\alpha} \qquad (11)$$

for $1 < \alpha < 2$ and $L_{max}, L_c >> L_{min}$. Obviously there are two limiting cases of the dependence of the total luminosity up on SFR, depending on whether $N(> L_c)$ exceeds unity. In the limit of low SFR (small number of sources), $L_{max} < L_c$ and the dependence might be strongly non-linear:

$$L_{total} \propto SFR^{\frac{1}{\alpha-1}} \qquad (12)$$

e.g. for $\alpha = 1.5$ the relation is quadratic $L_{total} \propto SFR^2$. For sufficiently large values of SFR, (large number of sources and, correspondingly, Gaussian probability distribution of the integrated luminosity), $L_{max} > L_c$ and the dependence is linear, in accord with eq.(8).

Interestingly, the entire existence of the linear regime in the L_X–SFR relation is a direct consequence of existence of the cut-off in the luminosity function. For a sufficiently flat luminosity function, $\alpha < 2$, the collective luminosity of the sources grows faster than linear law because more and more bright sources contribute to the total luminosity as the star formation rate increases. Only in the presence of the maximum possible luminosity of the sources, L_c (for instance Eddington limit for the neutron star) the regime can be reached, when $N(> L_c)$ becomes larger than unity and subsequent increase of the star formation rate results in the linear growth of the total luminosity. The position of the break in L_X–SFR relation depends on the slope of the luminosity function and the value of the cut-off luminosity:

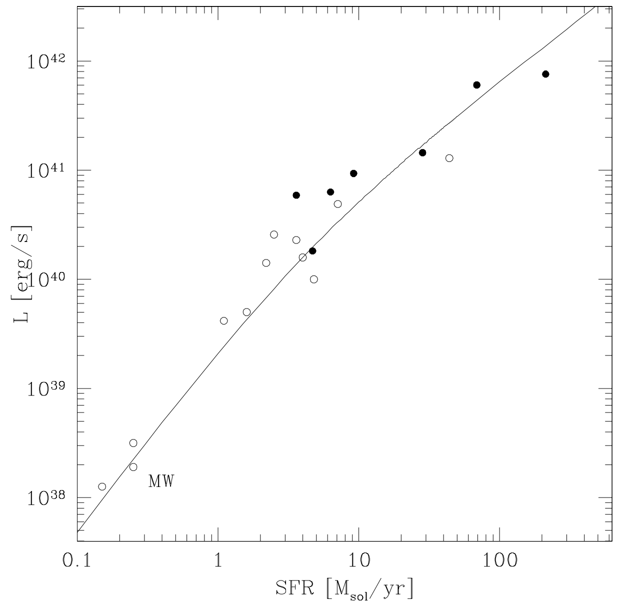

Figure 7. The total luminosity of the of the galaxies plotted vs. star formation rate. The open circles are the nearby galaxies from Table 1, the filled circles are distant (spatially unresolved) star forming galaxies from the Hubble Deep Field North. The thin solid line is defined by eq.(8) for low SFRs and eq.(19).

$$\mathrm{SFR}_{\mathrm{break}} \propto L_c^{\alpha-1} \qquad (13)$$

Combined with the slope of L_X–SFR relation in the low SFR regime (eq.(12)) this opens a possibility to constrain the parameters of the luminosity function studying the L_X–SFR relation alone, without actually constructing the luminosity functions, e.g. in distant unresolved galaxies.

The approximate relation between the most probable value of the total luminosity and SFR derived based on the above arguments and the luminosity function from eq.(6) is shown by the thin solid line in the Fig. 7. Sufficiently good agreement of the predicted $L_X - SFR$ relation with the data is obvious. Importantly, the predicted relation agrees with the data both in high and low SFR regime, thus giving an independent confirmation of existence of the cut-off in the luminosity function of HMXBs at $L_c \sim$ few $\times\ 10^{40}$ erg/s.

3.5 Hubble Deep Field North

In order to check whether the correlation, which is clearly seen from Fig. 7 for nearby galaxies, holds for more distant galaxies as well we used the data of the CHANDRA observation of the Hubble Deep Field North (Brandt et al. 2001). We cross correlated the list of the X-ray sources detected by CHANDRA with the catalog of radio sources detected by VLA at 1.4 GHz (Richards 2000). Using optical identifications of (Richards et al. 1998) and redshifts from Cohen et al. (2000) we compiled a list of galaxies detected by CHAN-

Table 3. Sample galaxies from the Hubble Deep Field North.

Source	redshift	$F_{1.4\ GHz}$ [μJy]	SFR [$M_\odot$/yr]	$S_{0.5-8\ keV}$ [10^{-15} erg/s/cm^2]	L_X [10^{40} erg/s]
123634.5+621213	0.458	233	28	0.43	14.4
123634.5+621241	1.219	230	213	0.3	75.9
123649.7+621313	0.475	49	8	0.15	2.5
123651.1+621030	0.410	95	9	0.3	9.3
123653.4+621139	1.275	66	69	0.22	6.3
123708.3+621055	0.423	45	4	0.18	5.9
123716.3+621512	0.232	187	5	0.18	1.8

DRA and classified as spiral or irregular/merger galaxies by Richards et al. (1998) and not known to show AGN activity. The K-correction for radio luminosity was done assuming power law spectrum and using the radio spectral indexes from Richards (2000). The X-ray luminosity was K-corrected and transformed to 2–10 keV energy range using photon indexes from Brandt et al. (2001). The final list of the galaxies selected is given in Table 3.

The star formation rates were calculated assuming that the non-thermal synchrotron emission due to electrons accelerated in supernovae dominates the observed 1.4 GHz luminosity and using the following relation from Condon (1992):

$$SFR_{radio} = 1.9 \cdot 10^{-29} \cdot \nu^{\alpha}_{\mathrm{G}Hz} \cdot L_\nu [\mathrm{erg/s/Hz}], \qquad (14)$$

where α is the slope of the non-thermal radio emission.

The galaxies from HDF North are shown in Fig.7 by the filled circles. A sufficiently good agreement with extrapolation of the Eq. (8) is obvious.

4 DISCUSSION

4.1 Neutron stars, stellar mass and intermediate mass black holes

Two well known and one possible types of the accreting objects should contribute to the X-ray luminosity function of the sources in star forming galaxies:

(i) the neutron stars
(ii) stellar mass black holes born due to collapse of high mass stars of well known types
(iii) intermediate mass ($50 \lesssim M/M_\odot \lesssim 10^5$) black holes of unknown origin.

In general case we should expect that each of these three types of accreting objects should have its own luminosity function depending on the mass distribution inside each class (more narrow for neutron stars, more broad for black holes and probably very broad for intermediate mass black holes), properties of the binary and mass loss type and rate from the normal star. In addition, each class of accreting objects is expected to have the maximum possible luminosity, close or exceeding by a factor of several the corresponding Eddington luminosity. Therefore, the combined luminosity function of a galaxy, containing all three types of objects should have several breaks. Such breaks are connected with a fact that, for example, below Eddington limit for a neutron star (or somewhat higher luminosity) more abundant neutron stars might dominate in the number of the objects, whereas at higher luminosities only black holes should contribute due to their higher masses and more broad mass distribution. Until now CHANDRA data did not show any evidence for the break in the luminosity function expected in the vicinity or above of Eddington luminosity for neutron star mass. However such a break must exist, the only question is how pronounced it is.

It is believed that the stars with masses higher that 60-100 $M_\odot$ are unstable. Therefore there should be an upper limit on the masses of the black holes born as result of a star collapse. It is natural that Eddington luminosity of these objects smoothed by the beaming effects should result in the maximum luminosity of the X-ray sources of this type.

The hypothetical intermediate mass black holes, probably reaching masses of $\sim 10^{3-5} M_\odot$, might be associated with extremely large star formation rates, black holes merging in dense stellar cluster etc., and are expected to be significantly less frequent than the ~stellar mass black holes. Therefore the transition from ~stellar mass black holes HMXBs luminosity function to the intermediate mass black holes must be much more visible in the cumulative luminosity function.

If the cut off in the luminosity function, observed at $\sim$ few $\times 10^{40}$ erg/s is real and if it corresponds to the maximum possible luminosity of the ~stellar mass black holes, it should lead to the drastic change in the slope of the L_X–SFR relation at extreme values of SFR. Possibly the observations of distant star forming galaxies with very high SFR is the best way to probe the population of intermediate mass black holes.

4.2 Other astrophysically important information

The good correlation between SFR and total X-ray luminosity due to HMXBs and the total number of HMXBs can obviously become a powerful and independent way to measure SFR in distant galaxies. In addition, this correlation is providing us with additional astrophysically important information:

- The luminosity function of HMXBs does not seem to depend strongly on the reason for the star formation event which might be completely different for the Milky Way and e.g. the Antennae where it is the result of tidal interaction of two galaxies.
- These data are proving that the neutron stars and black holes are produced in the star forming regions very efficiently and in very short time, proving the main predictions of stellar evolution.
- The luminosity functions provide information that binaries with different accretion rates (NS, BH) are distributed similarly in all galaxies of the sample available for study today.

• The existence of well separated X-ray sources is a way to look for small satellites of massive galaxies, like SMC.

5 CONCLUSION

Based on CHANDRA observations of nearby star forming galaxies and RXTE/ASM, ASCA and MIR-KVANT/TTM data on our Galaxy and Magellanic Clouds we studied the relation between star formation and the population of high mass X-ray binaries. Within the accuracy and completeness of the data available at present, we conclude that:

(1) The data are broadly consistent with the assumption that in a wide range of the star formation rates the luminosity distribution of HMXBs in a galaxy can be approximately described by a universal luminosity function, whose normalisation is proportional to the SFR (Fig.1,4,5). Although the accuracy of this approximation is yet to be determined based on a larger galaxies sample and deeper observations, we conclude from a rather limited sample available, that it might be of the order of $\sim 50\%$ or better.

In differential form the universal luminosity function can be approximated as a power law with a cut-off at $L_c \sim 2{\cdot}10^{40}$ erg/s:

$$\frac{dN}{dL_{38}} = 3.3 \cdot SFR \cdot L_{38}^{-1.6} \quad \text{for } L < L_c \tag{15}$$

where SFR is measured in units of $M_{\odot}$/yr and $L_{38} = L/10^{38}$ erg/sec. In cumulative form it is correspondingly:

$$N(>L_{38}) = 5.4 \cdot SFR \cdot (L_{38}^{-0.6} - 210^{-0.6}). \tag{16}$$

Although more subtle effects can not presently be excluded (and are likely to exist), we did not find strong non-linear dependences of the HMXB luminosity function on the SFR.

(2) Both the number and total luminosity of HMXBs in a galaxy are directly related to the star formation rate and can be used as an independent SFR indicator.

(3) The total number of HMXBs is directly proportional to SFR (Fig.3):

$$\mathrm{SFR}\ [M_{\odot}/\mathrm{yr}] = \frac{N(L > 2 \cdot 10^{38} \mathrm{erg/s})}{3.3}. \tag{17}$$

(4) The dependence of the total X-ray luminosity of a galaxy due to HMXBs up on SFR has a break at SFR≈ 4.4 $M_{\odot}$/yr.

At sufficiently high values of star formation rate, SFR$\gtrsim$4.4 $M_{\odot}$/yr ($L_{2-10\ \mathrm{keV}} \gtrsim 3 \cdot 10^{40}$ erg/s correspondingly) the X-ray luminosity of a galaxy due to HMXBs is directly proportional to SFR (Fig.7):

$$\mathrm{SFR}\ [M_{\odot}/\mathrm{yr}] = \frac{L_{2-10\ \mathrm{keV}}}{6.7 \cdot 10^{39}\ \mathrm{erg/s}} \tag{18}$$

At lower values of the star formation rate, SFR$\lesssim$4.4 $M_{\odot}$/yr ($L_{2-10\ \mathrm{keV}} \lesssim 3{\cdot}10^{40}$ erg/s) , the $L_X - SFR$ relation deviates from the linear law (Fig.7):

$$\mathrm{SFR}\ [M_{\odot}/\mathrm{yr}] = \left(\frac{L_{2-10\ \mathrm{keV}}}{2.6 \cdot 10^{39}\ \mathrm{erg/s}}\right)^{0.6} \tag{19}$$

The non linear $L_X - SFR$ dependence in the low SFR limit is caused by non-Gaussianity of the probability distribution of the integrated luminosity of a population of the discrete sources. We will give it more detailed and rigorous treatment in the forthcoming paper (Gilfanov et al. 2002).

(5) The position of the break in the $L_X - SFR$ relation depends on the cut-off luminosity L_c in the luminosity function of HMXB as $\mathrm{SFR}_{\mathrm{break}} \propto L_c^{\alpha-1}$, where α is differential slope of the luminosity function. Combined with the slope of L_X–SFR relation in the low SFR regime (eq.(12)) this opens a possibility to constrain the parameters of the luminosity function studying the L_X–SFR relation alone, without actually constructing the luminosity functions, e.g. in distant unresolved galaxies.

Agreement of the predicted $L_X - SFR$ relation with the data both in high and low SFR regime (Fig.7) gives an independent evidence for existence of the cut-off in the luminosity function of HMXBs at $L_c \sim$ few $\times\ 10^{40}$ erg/s.

(6) Based on the data of CHANDRA observations of the Hubble Deep Field North we showed, that the relation (18) between the SFR and the X-ray luminosity of a galaxy due to HMXBs holds for distant star forming galaxies with redshifts as high as $z = 1.2$ (Fig. 7).

REFERENCES

Armus L., Heckman T. M., Miley G. K., 1990, ApJ, 364, 471

Basko M. M., Sunyaev R. A., 1976, MNRAS, 175, 395

Bell E. F., Kennicutt R. C., 2001, ApJ, 548, 681

Bolton C. T., 1972, Nature Physical Science, 240, 124+

Brandt W. N., Alexander D. M., Hornschemeier A. E., Garmire G. P., Schneider D. P., Barger A. J., Bauer F. E., Broos P. S., Cowie L. L., Townsley L. K., Burrows D. N., Chartas G., Feigelson E. D., Griffiths R. E., Nousek J. A., Sargent W. L. W., 2001, AJ, 122, 2810

Buat V., Boselli A., Gavazzi G., Bonfanti C., 2002, A&A, 383, 801

Cohen J. G., Hogg D. W., Blandford R., Cowie L. L., Hu E., Songaila A., Shopbell P., Richberg K., 2000, ApJ, 538, 29

Condon J. J., 1992, ARA&A, 30, 575

David L. P., Jones C., Forman W., 1992, ApJ, 388, 82

de Vaucouleurs G., de Vaucouleurs A., Corwin H. G., Buta R. J., Paturel G., Fouque P., 1991, Third Reference Catalogue of Bright Galaxies. Volume 1-3, XII, 2069 pp. 7 figs.. Springer-Verlag Berlin Heidelberg New York

Eneev T. M., Kozlov N. N., Sunyaev R. A., 1973, A&A, 22, 41+

Eracleous M., Shields J. C., Chartas G., Moran E. C., 2002, ApJ, 565, 108

Fabbiano G., 1994, X-ray binaries. Cambridge University Press, p. 390

Feitzinger J. V., 1980, Space Science Reviews, 27, 35

Ghosh P., White N. E., 2001, ApJ, 559, L97

Gilfanov M., Grimm H.-J., Sunyaev R., 2002, in preparation

Gonzalez Delgado R. M., Perez E., 1996, MNRAS, 281, 1105

Griffiths R., Ptak A., Feigelson E., Garmire G., Townsley L., Brandt W., Sambruna R., Bregman J., 2000, Science, 290, 1325

Griffiths R. E., Padovani P., 1990, ApJ, 360, 483

Grimm H.-J., Gilfanov M., Sunyaev R., 2002, The Milky Way in X-rays for an outside observer. Log(N)-Log(S) and Luminosity Function of X-ray binaries from RXTE/ASM data, astro-ph/0109239
Holtzman J. A., Gallagher J. S., Cole A. A., Mould J. R., Grillmair C. J., Ballester G. E., Burrows C. J., Clarke J. T., Crisp D., Evans R. W., Griffiths R. E., Hester J. J., Hoessel J. G., Scowen P. A., Stapelfeldt K. R., Trauger J. T., Watson A. M., 1999, AJ, 118, 2262
Hoopes C. G., Walterbos R. . M., Bothun G. D., 2001, ApJ, 559, 878
Huchtmeier W. K., Richter O.-G., 1988, A&A, 203, 237
Kaaret P., 2001, ApJ, 560, 715
Kennicutt R. C., 1998, ARA&A, 36, 189
Kilgard R. E., Kaaret P. E., Krauss M. I., McDowell J. C., Prestwich A. H., Raley M. T., Zezas A., 2001, American Astronomical Society Meeting
King A., Davies M., Ward M., Fabbiano G., Elvis M., 2001, ApJ, 552, L109
Kuno N., Nakai N., 1997, PASJ, 49, 279
Lípari S., Díaz R., Taniguchi Y., Terlevich R., Dottori H., Carranza G., 2000, AJ, 120, 645
Lira P., Ward M., Zezas A., Alonso-Herrero A., Ueno S., 2002, MNRAS, 330, 259
Lyutyi V. M., Syunyaev R. A., Cherepashchuk A. M., 1973, Soviet Astronomy, 17, 1+
Madau P., Pozzetti L., 2000, MNRAS, 312, L9
Negishi T., Onaka T., Chan K.-W., Roellig T. L., 2001, A&A, 375, 566
Paczynsky B., Wiita P., 1980, A&A, 88, 23
Persic M., Salucci P., 1988, MNRAS, 234, 131
Ptak A., Griffiths R., White N., Ghosh P., 2001, ApJ, 559, L91
Ranalli P., Comastri A., Setti G., 2002, The 2–10 keV luminosity as a star formation rate indicator, astro-ph/0202241
Richards E. A., 2000, ApJ, 533, 611
Richards E. A., Kellermann K. I., Fomalont E. B., Windhorst R. A., Partridge R. B., 1998, AJ, 116, 1039
Rosa-Gonzalez D., Terlevich E., Terlevich R., 2002, An Empirical Calibration of Star Formation Rate Estimators, accepted by MNRAS
Roussel H., Sauvage M., Vigroux L., Bosma A., 2001, A&A, 372, 427
Sandage A., Tammann G. A., 1980, A revised Shapley-Ames Catalog of bright galaxies. Washington: Carnegie Institution, 1980, Preliminary version
Schreier E., Giacconi R., Gursky H., Kellogg E., Tananbaum H., 1972, ApJ, 178, L71
Shakura N., Sunyaev R., 1973, A&A, 24, 337
Sharina M. E., Karachentsev I. D., Tikhonov N. A., 1996, A&AS, 119, 499
Smith D. A., Wilson A. S., 2001, ApJ, 557, 180
Sofue Y., Reuter H.-P., Krause M., Wielebinski R., Nakai N., 1992, ApJ, 395, 126
Soria R., Kong A. K., 2002, XMM-Newton observations of the spiral galaxy M 74 (NGC 628), astro-ph/0203345
Soria R., Wu K., 2002, A&A, 384, 99
Syunyaev R., Gilfanov M., Churazov E., Loznikov V., Yamburenko N., Skinner G. K., Patterson T. G., Willmore A. P., Emam O., Brinkman A. C., Heise J., Intzand J., Jager R., 1990, Soviet Astronomy Letters, 16, 55+
Tananbaum H., Gursky H., Kellogg E., Giacconi R., Jones C., 1972, ApJ, 177, L5+
Terashima Y., Wilson A., 2002, Ultraluminous X-ray sources in M51, astro-ph/0204321
Toomre A., Toomre J., 1972, ApJ, 178, 623
Verbunt F., van den Heuvel E., 1994, X-ray binaries. Cambridge University Press, p. 457
Wilkinson M. I., Evans N. W., 1999, MNRAS, 310, 645
Yokogawa J., 2002, PhD thesis, Kyoto University
Young J. S., Allen L., Kenney J. D. P., Lesser A., Rownd B., 1996, AJ, 112, 1903
Zezas A., Fabbiano G., Rots A., Murray S., 2002, Chandra observations of "The Antennae" galaxies (NGC4038/39): II. Detection and analysis of galaxian X-ray sources, astro-ph/0203174